

## An X-Ray Investigation of the Hydrolysis Products of Tin(II) in Solution

GEORG JOHANSSON and HITOSHI OHTAKI\*

*Department of Inorganic Chemistry, Royal Institute of Technology,  
S-100 44 Stockholm 70, Sweden*

The X-ray scattering from hydrolyzed and acid water solutions of 3 M tin(II) perchlorate has been measured. In its inner coordination sphere the tin(II) ion has between two and three water molecules at distances of 2.3 Å. In the hydrolyzed solutions polynuclear complexes are formed with Sn-Sn distances between 3.6 Å and 4 Å. In the most hydrolyzed of the solutions investigated the average number of Sn atoms bonded to each other Sn atom is about 1.5. Possible structures for the complexes are discussed.

The hydrolytic reactions of the tin(II) ion have been investigated by several workers.<sup>1-7</sup> The emf measurements by Tobias,<sup>7</sup> which were made in a 3 M (Na)ClO<sub>4</sub> medium with tin concentrations varying from 2.50 mM to 40 mM, led to the conclusion that the main hydrolysis product is the tri-nuclear Sn<sub>3</sub>(OH)<sub>4</sub><sup>2+</sup> with some minor products, Sn<sub>2</sub>(OH)<sub>2</sub><sup>2+</sup> and SnOH<sup>+</sup>, also formed. It is interesting to compare this with results reported for lead(II), where the tetra-nuclear Pb<sub>4</sub>(OH)<sub>4</sub><sup>4+</sup> or the hexa-nuclear Pb<sub>6</sub>(OH)<sub>8</sub><sup>4+</sup> are predominant in the whole accessible concentration range, with the complexes Pb<sub>3</sub>(OH)<sub>4</sub><sup>2+</sup> and Pb<sub>2</sub>OH<sup>3+</sup> formed in lower concentrations.<sup>8-10</sup>

In the solid state tin(II) and lead(II) seem to form closely related hydrolysis complexes, which can be pictured as based on a group of three metal atoms arranged in a triangle with an oxygen atom slightly above the center of the triangle. By the sharing of edges these triangles combine into tetrahedra or octahedra of metal atoms. Crystals of the basic tin(II) sulfate, Sn<sub>2</sub>OSO<sub>4</sub>, have been reported to be built up from discrete complexes with eight tin atoms.<sup>11</sup> They can be described as a basic tetrahedron of tin atoms sharing its faces with four similar tetrahedra. A related structure has been found for the basic lead(II) perchlorate, Pb<sub>6</sub>O(OH)<sub>6</sub>(ClO<sub>4</sub>)<sub>4</sub>·H<sub>2</sub>O, in which a tetrahedron of lead atoms shares two of its faces with other tetrahedra leading to hexa-nuclear complexes, Pb<sub>6</sub>O(OH)<sub>6</sub><sup>4+</sup>.<sup>12</sup> In recent structure determinations of Sn<sub>6</sub>O<sub>4</sub>(OH)<sub>4</sub>

\* Present address: Tokyo Institute of Technology, O-okayama, Meguro-ku, Tokyo, Japan.

and the isomorphous lead(II) compound, octahedra of metal atoms have been found to occur.<sup>13,14</sup>

An X-ray investigation of hydrolyzed lead(II) perchlorate solutions<sup>15</sup> has shown that the hexa-nuclear complex  $\text{Pb}_6\text{O}(\text{OH})_6^{4+}$  retains its structure in solution and that the tetra-nuclear complex has a tetrahedral arrangement of lead atoms. In view of the closely related structures of tin(II) and lead(II) in the solid state it was of interest to make a similar X-ray investigation of hydrolyzed tin(II) solutions, although tin, because of its lower atomic number, is far less suitable than lead for such an investigation.

As in previous investigations of this kind<sup>15-18</sup> a series of solutions with constant metal ion concentration but with varying degrees of hydrolysis has been investigated. Variations in the X-ray scattering between the different solutions are then mainly due to the formation of hydrolysis complexes and can be interpreted in terms of interatomic distances within the complexes and frequencies of these distances.

### EXPERIMENTAL

*Preparation of solutions.* Partially hydrolyzed tin(II) perchlorate solutions were prepared by addition of  $\text{NaHCO}_3$  to tin(II) perchlorate solutions which were prepared by a modification of the method described by Noyes and Toabe.<sup>19</sup> A schematic diagram of the apparatus used for the preparation of the solutions is shown in Fig. 1.

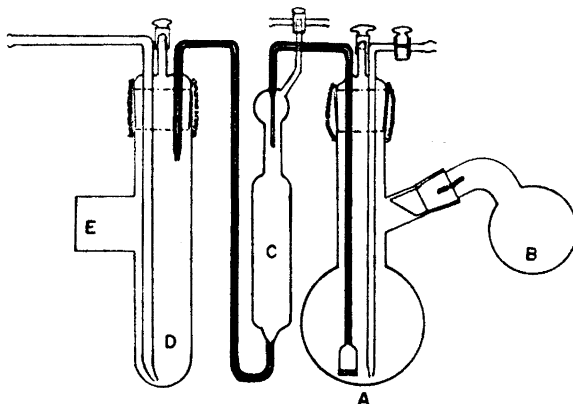


Fig. 1. The apparatus used for the preparation of the tin(II) perchlorate solution.

Granular metallic tin (*p.a.* grade of a purity better than 99.5 %) was washed three times with dilute hydrochloric acid, then with water, and finally with alcohol. The granules were dried by pressing them between sheets of filter paper and were then transferred to the bulb A (Fig. 1). The apparatus was evacuated until the metal granules were completely dried. A slightly acid copper perchlorate solution was placed in the bulb B. The air initially in the apparatus was completely replaced with argon by repeated evacuation and back-filling with pure argon. By turning the bulb B the copper perchlorate solution was then transferred to the bulb A. The displacement of the copper ions by tin was completed within a few hours. Occasional shaking of the apparatus was effective in speeding up the exchange reaction and in preventing the granules sticking. The resulting solu-

tion was clear with a pale greenish yellow color. It was transferred through a tube with a glass filter into a calibrated buret (C). About 30 ml of the solution was then transferred by means of argon gas into the tube D in which a weighed amount of  $\text{NaHCO}_3$  powder had been placed at E. The resulting solution was transferred through a glass tube into a glass vessel which was placed in the X-ray diffractometer. During the preparation and the transfer of the solution it was not in contact with any stop-cock or with air. Tests for copper and for chloride in the solution were negative.

Copper perchlorate was prepared by dissolving copper(II) oxide (Merck, *p.a.*) in reagent grade perchloric acid. The crystals obtained were recrystallized three times from water.

*Analysis of solutions.* The determination of tin(II) was made according to Jamieson.<sup>20</sup> An aliquot of the tin perchlorate solution was transferred to an Erlenmeyer flask in which 30 ml of hydrochloric acid, 20 ml of water, and 2–4 ml of chloroform were contained. The solution was titrated with a standard potassium iodate solution. The titration was continued with thorough shaking of the stoppered flask after each addition of potassium iodate solution until the end point was reached.

A Gran plot<sup>21</sup> of the emf values measured when acidifying the hydrolyzed solution was used for the evaluation of the analytical hydrogen ion excess in the solution.

The total amount of perchlorate was determined with a cation exchange resin. The titration of the free acid was made with a standard sodium hydroxide solution.

The concentration of sodium ions was determined from the material balance of ions in the solution. The density of a solution was determined pycnometrically.

The compositions of the solutions investigated are given in Table 1. The values  $\bar{n}$ , given in the table, represent the number of OH groups per Sn atom as estimated from

Table 1. Concentrations of solutions. The volume of a stoichiometric unit of solution =  $V \text{ \AA}^3$ .

Solution No. Concentration	I ( $V = 503.5 \text{ \AA}^3$ )		II ( $V = 533.4 \text{ \AA}^3$ )		III ( $V = 555.3 \text{ \AA}^3$ )	
	g atoms/l	atoms/unit volume	g atoms/l	atoms/unit volume	g atoms/l	atoms/unit volume
Sn	3.298	1	3.113	1	2.990	1
Cl	6.825	2.070	6.431	2.067	6.422	2.148
O	67.07	20.34	65.20	20.95	65.34	21.85
H	77.77	24.19	77.34	24.85	76.97	25.74
Na			1.788	0.574	2.789	0.933
$\bar{n}$		0		0.507		0.785

the hydrogen ion excess. Precipitates were formed in a 3 M solution when the value of  $\bar{n}$  exceeded 0.8. Increase of the Sn(II) concentrations led to lower maximum  $\bar{n}$  values. In chloride solutions the maximum values of  $\bar{n}$  that could be obtained were lower than those in perchlorate solutions.

*Measurements of the X-ray scattering.* The diffractometer was the same as described in previous papers.<sup>17,22</sup> A glass vessel with a diameter of 40 mm and a depth of 10 mm was used to hold the solution. It was enclosed in an airtight sample holder through which a slow stream of argon gas was passed.

$\text{MoK}\alpha$  radiation ( $\lambda = 0.7108 \text{ \AA}$ ) was used for all the measurements. A focusing  $\text{LiF}$  monochromator was placed between the sample and the scintillation counter. Further monochromatization was performed by means of a pulse height discriminator. The opening slits used were  $1/12^\circ$ ,  $1/4^\circ$ , and  $1^\circ$ . Scaling factors to convert all measured data to the same opening slit were obtained from measurements in overlapping regions. Points were measured at intervals of  $0.1^\circ$  in  $\theta$  up to  $\theta = 6^\circ$ , and  $0.25^\circ$  to  $\theta = 70^\circ$ , the largest angle obtainable. Usually 40 000 counts were taken for each point, which corresponds to a statistical error of 0.5 %. A number of points were measured repeatedly in order to detect and to correct for any long time variations in the equipment. A Philips PW-1130 X-ray unit was employed for the measurements. Background radiation was determined by covering the receiving slit with a lead plate.

Table 2. Observed intensity values as a function of  $s = 4\pi \sin \theta / \lambda$  for the three solutions investigated.  $I$  is the observed intensity after correction for polarization, scaling, and subtraction of incoherent radiation. The reduced intensity values  $i(s)$  are also given.

I			II			III			I			II			III		
$s$	$I$	$i$	$s$	$I$	$i$	$s$	$I$	$i$	$s$	$I$	$i$	$s$	$I$	$i$	$s$	$I$	$i$
0.400	1534	-2809.1	2.457	-1939.3	2724	-1877.6	5.010	1219	32.1	1206	7.6	1209	-6.4				
0.451	1587	-2742.6	2.460	-1922.5	2784	-1802.5	5.084	1195	30.9	1193	17.0	1195	2.8				
0.481	1637	-2677.6	2.465	-1900.3	2780	-1730.1	5.158	1176	34.5	1187	33.5	1198	29.9				
0.512	1771	-2527.1	2.507	-1845.8	2736	-1816.8	5.232	1160	39.8	1179	47.9	1191	44.9				
0.543	1800	-2481.4			2769	-1765.0	5.305	1140	39.9	1172	62.0	1177	52.7				
0.574	1865	-2399.5	2.620	-1695.9		-1699.2	5.379	1111	37.0	1147	57.3	1197	54.0				
0.605	1925	-2321.1			2764	-1731.7	5.452	1096	35.3	1126	59.3	1194	51.1				
0.636	1997	-2250.1	2.656	-1621.8	2717	-1757.3	5.526	1086	44.2	1110	59.3	1121	57.5				
0.666	2120	-2087.4			2701	-1752.1	5.599	1072	47.6	1081	48.7	1102	58.1				
0.682			2.611	-1656.9			5.672	1046	39.8	1065	48.4	1084	58.5				
0.697	2222	-1956.1	2.563	-1668.4	2697	-1753.6	5.745	1025	36.1	1046	48.7	1072	63.9				
0.728	2275	-1893.8	2.561	-1654.4	2615	-1793.3	5.818	1018	45.1	1026	45.5	1044	54.1				
0.759	2369	-1776.7	2.549	-1644.1	2572	-1812.3	5.891	999	42.5	1012	47.7	1029	55.8				
0.790	2362	-1760.6	2.540	-1731.1	2511	-1849.3	5.963	977	36.0	989	40.9	1001	45.8				
0.821	2419	-1681.4	2.495	-1652.6	2445	-1889.8	6.036	960	33.4	966	33.1	975	35.1				
0.836			2.451	-1684.3			6.108	946	34.4	948	29.7	956	29.5				
0.851	2484	-1593.2			2445	-1864.9	6.181	940	42.7	929	25.2	936	24.9				
0.882	2475	-1578.0	2.460	-1639.5	2394	-1890.1	6.253	921	37.2	912	22.1	918	20.3				
0.913	2529	-1499.5	2.445	-1629.2	2384	-1873.1	6.325	901	29.9	894	18.3	895	9.8				
0.944	2558	-1445.8	2.431	-1618.6	2359	-1870.9	6.397	882	24.1	880	16.6	881	10.6				
0.975	2612	-1367.0	2.442	-1581.3	2377	-1826.0	6.469	850	14.6	859	8.9	852					
0.990			2.458	-1553.2			6.541	844	10.0	843	5.2	844	-0.8				
1.006	2636	-1316.5	2.502	-1495.5	2345	-1830.3	6.612	829	6.9	829	2.9	838	5.7				
1.036	2660	-1266.8	2.533	-1438.0	2362	-1784.9	6.684	808	-2.8	812	-1.9	816	-4.7				
1.067	2774	-1126.5	2.550	-1395.0	2375	-1745.5	6.755	789	-10.5	797	-6.2	802	-6.9				
1.098	2776	-1097.5	2.565	-1352.4	2396	-1694.0	6.826	774	-14.3	787	-4.9	785	-13.2				
1.129	2811	-1035.7	2.610	-1280.0	2403	-1657.6	6.897	774	-7.4	775	-6.3	777	-9.6				
1.160	2895	-924.4	2.624	-1236.4	2448	-1582.5	6.968	747	-20.8	758		758	-8.4				
1.190	2932	-858.8	2.677	-1156.7	2498	-1503.3	7.039	742	-15.7	749	-11.9	756	-10.0				
1.221	2991	-771.8	2.718	-1087.7	2510	-1461.3	7.110	729	-19.0	737	-13.6	742	-14.6				
1.252	3039	-696.1	2.747	-1030.2	2551	-1389.7	7.180	711	-27.5	723	-18.1	732	-14.1				
1.283	3078	-628.3	2.807	-941.6	2617	-1293.5	7.251	705	-24.0	706	-25.7	722	-14.3				
1.298			2.808	-925.7			7.321			700	-23.0	707	-20.3				
1.313	3124	-553.7			2.663	-1216.5	7.391	682	-28.8	687	-26.5	692	-26.5				
1.344	3213	-436.0	2.888	-802.0	2713	-1135.7	7.461	672	-30.2	681		685	-23.7				
1.375	3240	-379.6	2.954	-706.8	2734	-1082.6	7.531	661	-33.0	659	-27.1	674	-26.7				
1.406	3295	-295.9	2.996	-635.7	2854	-951.7	7.601	654	-31.1	655	-32.6	663	-28.4				
1.437	3345	-216.4	3.083	-519.2	2926	-828.3	7.671	644	-33.3	646	-32.7	652	-30.7				
1.452			3.100	-487.5			7.740	639	-29.6	642	-28.5	648	-26.3				
1.457	3441	-91.4	3.185	-387.5	3027	-696.4	7.809	635	-25.8	630	-31.9	637	-28.8				
1.498	3431	-71.3	3.724	-268.5	3119	-573.3	7.879	626	-26.6	627	-27.8	633	-25.6				
1.529	3474	1.0	3.346	-166.8	3220	-439.9	7.947	626	-25.0	621	-25.5	625	-27.5				
1.560			3.520	36.1			8.016	614	-22.9	612	-27.2	613	-29.5				
1.590			3.543	89.6	3381	-216.1	8.085	613	-16.9	604	-27.2	602	-32.5				
1.606	3657	258.7					8.154	605	-19.0	602	-22.0	601	-26.6				
1.621			3.602	178.1	3531	-34.9	8.222	601	-14.2	599	-17.3	595	-24.8				
1.652			3.665	271.7			8.290	606	-2.5	593	-15.8	593	-19.5				
1.682	3678	354.6	3.752	388.9	3831	327.9	8.358	596	-5.3	591	-11.4	592	-13.7				
1.713			3.818	483.9	3859	388.4	8.426	585	-11.5	586	-9.0	587	-11.2				
1.744			3.834	530.6			8.494	585	-2.2	581	-7.7	584	-7.3				
1.759	3655	406.4	3.883	593.7			8.561	577	-5.8	579	-2.9	583	-1.9				
1.775			3.862	580.1	3951	544.1	8.629	578	3.2	575	-0.4	575	-3.4				
1.805			3.825	581.7			8.696	566	-1.5	572	2.6	574	1.8				
1.836	3517	342.4	3.762	548.2	3997	652.8	8.763	569	7.4	567	4.8	570	4.7				
1.913	3348	247.7	3.695	485.7	3958	675.4	8.830	560	4.8	565	6.3	564	5.0				
1.989	3128	100.8	3.415	349.7	3704	518.2	8.897	558	0.9	560	3.8	560	6.3				
2.066	2869	-85.5	3.120	128.6	3416	307.5	8.963	550	5.8	556	11.0	561	13.7				
2.143	2658	-224.5	2.886	-33.5	3102	70.7	9.030	552	14.1	549	10.0	552	10.8				
2.219	2551	-281.6	2.670	-178.1	2849	-107.0	9.096	535	3.0	542	8.7	544	7.6				
2.296	2410	-335.5	2.533	-245.4	2656	-225.3	9.162	541	15.6	539	10.7	543	12.9				
2.372	2328	-347.9	2.387	-322.8	2520	-289.0	9.228	529	7.2	532	9.5	538	12.7				
2.449	2287	-322.4	2.304	-338.9	2450	-287.8	9.294	529	13.0	528	10.5	535	14.9				
2.525	2268	-277.3	2.241	-336.7	2347	-321.1	9.359	519	7.7	526	13.8	527	18.1				
2.601	2288	-195.8	2.208	-305.6	2275	-325.7	9.425	510	4.4	519	12.2	527	18.1				
2.678	2273	-147.1	2.168	-262.3	2207	-286.5	9.490	507	6.6	505		516	12.0				
2.754	2279	-80.6	2.166	-223.3	2207	-286.5	9.555	500	3.8	506	3.1	501	6.4				
2.830	2253	-47.6	2.148	-184.3	2100	-182.7	9.620	501	9.7	496		510	10.8				
2.906	2232	-11.2	2.143	-129.4	2162	-182.7	9.684	494	8.0	489	1.3	498	8.7				
2.982	2202	14.3	2.128	-88.2	2131	-154.4	9.749	488	6.1	489	5.9	486	1.2				
3.058	2169	35.9	2.105	-56.2	2124	-103.5	9.813	481	3.7	480	1.7	483	3.0				
3.134	2132	51.6	2.074	-34.3	2098	-73.1	9.877	475	2.7	478	4.2	480	3.9				
3.210	2086	96.5	2.052	-7.7	2077	-39.2	9.941	469	0.8	470	1.0	477	5.7				
3.286			2.018	12.2	2048	-14.7	10.005	467	3.4	462	-2.5	465	-4.2				
3.362	1958	26.1	1.984	26.8	2032	20.1	10.068	460	0.6	460	-0.4	461	-2.0				
3.437	1891	6.7	1.935	23.0	1997	35.7	10.132	452	-2.7	455	-1.6	458	-1.1				
3.513	1834	-5.1	1.877	15.5	1955	42.3	10.195	451	0.0	452	0.0	451	-3.4				
3.589	1756	-35.9	1.803	1.4	1905	39.0	10.2585										

Table 2. Continued.

I			II			III			I			II			III		
s	I	1	s	I	1	s	I	1	s	I	1	s	I	1	s	I	1
11.415	383	5.0	383	2.4	383	-0.6	14.233	263	3.2	258	4.9	273	4.5	273	4.5	273	4.5
11.474	376	0.6	378	0.3	378	-4.6	14.343	265	6.1	256	4.4	271	4.5	271	4.5	271	4.5
11.533	370	-2.2	376	1.3	374	-3.5	14.589	263	5.4	267	6.3	263	5.3	263	5.3	263	5.3
11.591	372	2.5	371	-0.9	367	-7.7	14.432	261	5.6	265	6.0	268	5.8	268	5.8	268	5.8
11.649	367	0.8	367	-1.5	367	-4.9	14.477	259	4.9	263	5.7	263	5.7	263	5.7	263	5.7
11.707	363	-0.1	365	-0.5	365	-3.2	14.521	256	3.2	261	5.3	259	7.9	259	7.9	259	7.9
11.765	363	2.4	362	-0.9	363	-5.7	14.565	257	5.0	258	3.5	265	6.6	265	6.6	265	6.6
11.822	356	-1.4	354	-5.6	362	-1.6	14.609	255	4.7	258	4.4	263	5.0	263	5.0	263	5.0
11.879	350	-4.6	355	-2.9	359	-1.9	14.652	253	4.0	258	5.6	263	6.3	263	6.3	263	6.3
11.936	349	-3.5	349	-5.5	355	-5.3	14.695	256	6.8	256	5.5	262	6.7	262	6.7	262	6.7
11.993	346	-3.7	348	-4.4	349	-6.9	14.738	248	1.6	255	4.2	258	3.7	258	3.7	258	3.7
12.050	339	-7.8	344	-5.5	349	-4.6	14.780	252	6.8	252	3.6	260	6.6	260	6.6	260	6.6
12.106	340	-4.4	340	-7.0	342	-9.0	14.821			251	3.8						
12.162	337	-4.6	339	-5.6			14.862	248	4.3			256	4.8	256	4.8	256	4.8
12.218	332	-5.9	337	-4.4	339	-8.5	14.904	247	4.9	248	2.8	258	7.5	258	7.5	258	7.5
12.274	331	-5.8	335	-6.5	337	-7.0	14.905	245	3.7	249	4.8	252	3.2	252	3.2	252	3.2
12.329	329	-5.3	329	-7.3	335	-7.9	14.947	242	2.0	246	3.2	254	6.2	254	6.2	254	6.2
12.384	322	-9.4	326	-7.9	330	-8.8	14.988	243	4.9	245	3.1	249	5.1	249	5.1	249	5.1
12.439	321	-8.7	325	-6.8	330	-6.5	15.029	241	3.4	244	3.7	248	2.8	248	2.8	248	2.8
12.494	316	-11.0	325	-4.4	328	-8.0	15.070	238	2.1	243	2.7	247	3.6	247	3.6	247	3.6
12.549	313	-11.1	322	-5.1	323	-7.2	15.110	239	4.2	239	1.5	246	3.5	246	3.5	246	3.5
12.603	310	-12.1	318	-6.9	325	-4.9	15.150	236	1.9	238	1.2	245	3.7	245	3.7	245	3.7
12.657	312	-8.4	317	-5.7	321	-4.5	15.189	235	2.7	236	0.9	242	1.8	242	1.8	242	1.8
12.711	305	-12.8	316	-4.4	323	-2.5	15.229	234	2.6	236	1.9	240	1.4	240	1.4	240	1.4
12.764	308	-7.8	314	-4.1	321	-2.1	15.268	233	2.7	235	1.6	238	0.4	238	0.4	238	0.4
12.817	305	-8.2	312	-4.5	316	-4.9	15.307	232	2.4	235	0.9	238	5.1	238	5.1	238	5.1
12.870	302	-9.1	311	-2.9	318	-1.5	15.345	230	1.9	232	1.0	235	-0.5	235	-0.5	235	-0.5
12.923	301	-8.5	305	-7.0	313	-0.9	15.383	228	1.4	230	0.4	234	0.5	234	0.5	234	0.5
12.976	301	-6.3			312	-2.7	15.421	230	4.0	228	0.0	233	-0.1	233	-0.1	233	-0.1
13.028	298	-6.8	303	-5.0	305		15.459	227	2.8	226	-1.0	231	0.0	231	0.0	231	0.0
13.080	296	-7.2	302	-4.4	307	-3.3	15.495	225	1.8	226	-0.5	229	-1.0	229	-1.0	229	-1.0
13.132	296	-4.5	302	-2.0	307	-2.5	15.533	224	1.4	225	0.1	229	0.1	229	0.1	229	0.1
13.183	295	-4.3	298	-4.5	305	-4.5	15.570	222	0.9	223	-1.1	227	-0.7	227	-0.7	227	-0.7
13.235	291	-5.2	296	-4.1	303	-2.5	15.606	220	-0.1	223	0.3	225	-1.5	225	-1.5	225	-1.5
13.286	292	-2.8			300	-3.1	15.642	220	1.0	221	-1.3	225	-0.7	225	-0.7	225	-0.7
13.338	292	-1.3	293	-3.8	293	-2.5	15.678	217	-1.4	217	-3.5	224	-0.3	224	-0.3	224	-0.3
13.387	287	-4.2	291	-3.2	300	-0.2	15.714	217	-0.2	218	-2.0	222	-1.2	222	-1.2	222	-1.2
13.437	287	-2.1	291	-1.9	298	-2.3	15.749	217	0.6	217	-1.6	221	-1.6	221	-1.6	221	-1.6
13.487	288	0.0	289	-2.0	294	-2.5	15.784	216	0.4	215	-2.7	221	-0.8	221	-0.8	221	-0.8
13.537	285	-0.5	289	-0.5	293	-1.8	15.818	215	-1.0	214	-2.5	218	-3.0	218	-3.0	218	-3.0
13.586	283	-0.8	285	-1.9	291	-1.7	15.855	212	-1.9	212	-3.5	217	-2.7	217	-2.7	217	-2.7
13.636	285	2.9	284	-1.4	290	-0.3	15.887	210	-2.2	212	-2.9	215	-3.7	215	-3.7	215	-3.7
13.685	285	4.9	284	0.4	291	2.7	15.920	208	-3.7	211	-2.5	213	-4.1	213	-4.1	213	-4.1
13.733	281	2.3	283	0.5	291	3.5	15.954	208	-2.7	210	-3.3	213	-3.9	213	-3.9	213	-3.9
13.780	273	2.3	280	0.0	285	-3.7	15.987	207	-5.1	208	-5.5	211	-4.7	211	-4.7	211	-4.7
13.830	279	4.0	279	0.6	286	1.5	16.020	207	-2.2	207	-3.6	208	-6.2	208	-6.2	208	-6.2
13.878	277	2.9	280	2.3	283	2.0	16.052	205	-5.3	205	-4.3	207	-5.2	207	-5.2	207	-5.2
13.926	275	3.1	277	1.4	281	3.0	16.085	202	-5.3	205	-4.3	207	-5.8	207	-5.8	207	-5.8
13.973	277	6.2	275	1.3	280	0.8	16.116	204	-2.1			206	-5.2	206	-5.2	206	-5.2
14.020	274	4.9	278	5.7	280	2.0	16.148	204	-1.7	202	-5.1	208	-4.7	208	-4.7	208	-4.7
14.067	272	5.0	274	3.4	281	4.5	16.179	200	-4.9	201	-5.8	205	-4.4	205	-4.4	205	-4.4
14.114	271	5.2	274	4.4	278	3.3	16.210	200	-3.6	200	-5.9	202	-7.1	202	-7.1	202	-7.1
14.160	270	5.7	275	2.5	278	4.5	16.241	198	-4.9	200	-4.3	201	-6.4	201	-6.4	201	-6.4
14.206	269	5.6	273	4.2	275	4.8	16.271	199	-3.2	199	-5.7	201	-5.5	201	-5.5	201	-5.5
14.252	265	4.7	267	2.0	276	5.9	16.301	195	-5.8	195	-3.5	197	-8.7	197	-8.7	197	-8.7

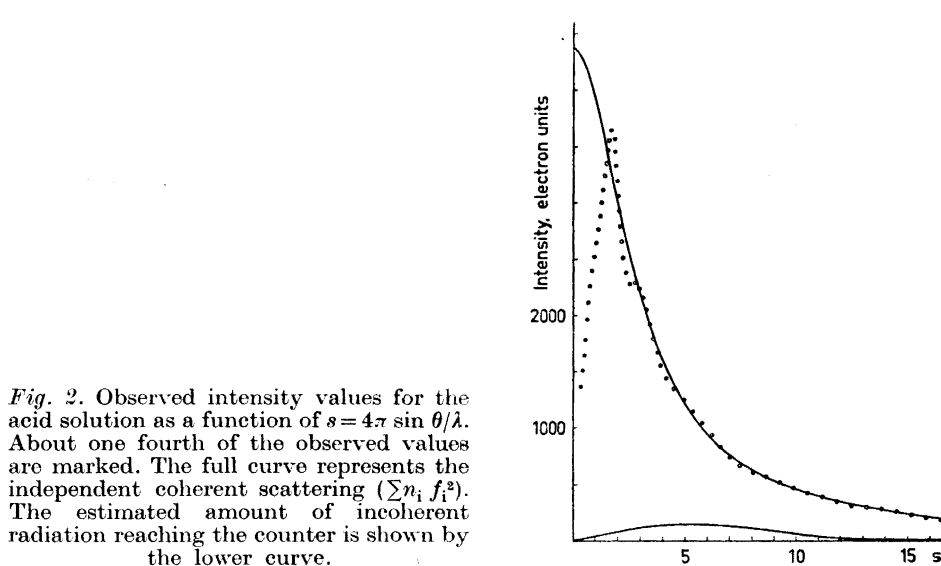


Fig. 2. Observed intensity values for the acid solution as a function of  $s = 4\pi \sin \theta / \lambda$ . About one fourth of the observed values are marked. The full curve represents the independent coherent scattering ( $\sum n_i f_i^2$ ). The estimated amount of incoherent radiation reaching the counter is shown by the lower curve.

*Treatment of the data.* The data were treated in the same way as described in a previous paper.<sup>17</sup> The scattering factors used were those given by Cromer and Waber<sup>23</sup> for the neutral atoms. Anomalous dispersion corrections ( $\Delta f'$  and  $\Delta f''$ ) were applied according to Cromer<sup>24</sup> for Sn, Cl, and Na. The incoherent scattering was estimated from the values given in the International Tables<sup>25</sup> for Cl, O, and Na, from the values given by Compton and Allison<sup>26</sup> for H, and from the formula given by Bewilogua<sup>27</sup> for Sn. The amount of incoherent radiation passing through the monochromator was estimated from the spectrum of the X-ray tube as described previously.<sup>17,22</sup> At the largest scattering angles it was determined by measurements with a zirconium filter. After correction for polarization in the solution and in the monochromator the outermost part of the measured intensity curve ( $\theta > 35^\circ$ ) was used for the scaling, which was done by comparing observed intensity values with the sum of the independent coherent scattering ( $\sum n_i f_i^2$ ) and the incoherent scattering. The scaled intensity values were corrected for the incoherent radiation and reduced intensities were then obtained by subtracting the independent coherent scattering. All calculations were referred to a stoichiometric unit of solution corresponding to the volume containing one Sn atom (Table 1).

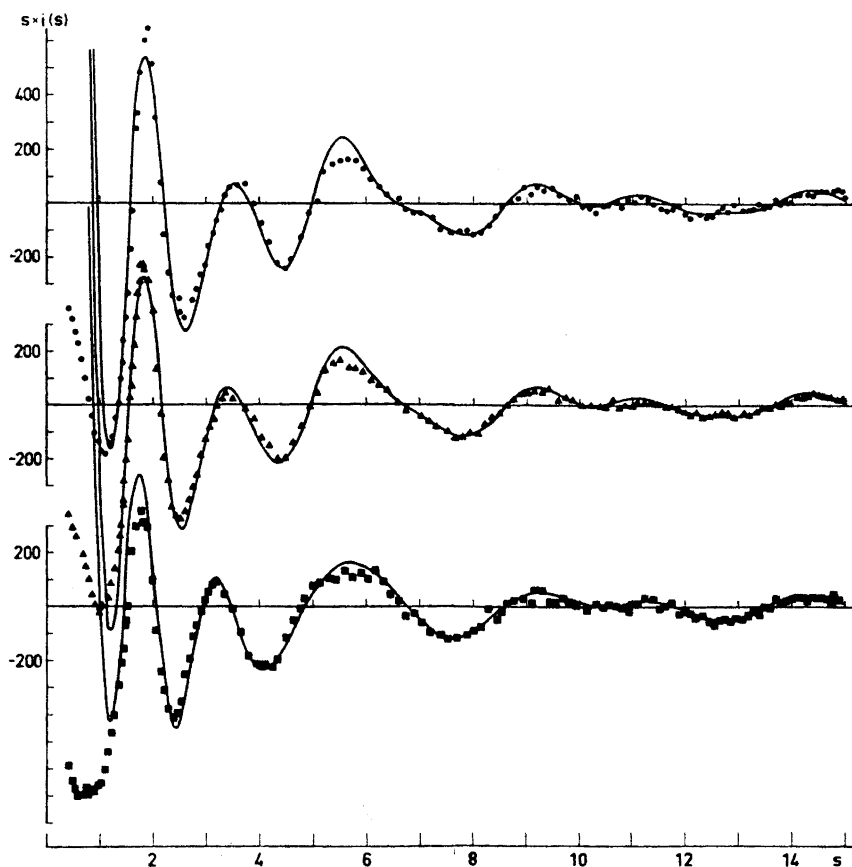


Fig. 3. Values  $s \cdot i(s)$  for the three solutions investigated. Every second point has been marked. The full curves are calculated values obtained with the use of the parameters from the least squares refinements (Table 3) and the analysis of the difference curves (last column in Table 4). The lower curve represents the acid solution (I) and the upper curve the most hydrolyzed of the solutions (III).

The measured intensity values after corrections for polarization, scaling, and subtraction of incoherent radiation are given in Table 2 and in Fig. 2, as a function of  $s = 4\pi \sin \theta/\lambda$ . The corresponding values of the reduced intensities  $i(s)$  are given in Table 2 and the  $s \cdot i(s)$  values in Fig. 3 after correction for spurious peaks below 1 Å in the radial distribution curves as described in previous papers.<sup>17,18</sup>

The radial distribution curves were calculated from the reduced intensity values according to the expression:

$$D(r) = 4\pi r^2 \rho_0 + 2r\pi^{-1} \int_0^{s_{\max}} i(s) [f_{\text{Sn}}(0)/f_{\text{Sn}}(s)]^2 \exp(-ks^2) \sin(rs) ds$$

In the sharpening factor,  $[f_{\text{Sn}}(0)/f_{\text{Sn}}(s)]^2 \exp(-ks^2)$ , the  $f_{\text{Sn}}(s)$  represents the scattering factor of Sn for a value  $s (= 4\pi \sin \theta/\lambda)$ . The value of  $k$  was chosen to be 0.01.

All calculations were carried out on an IBM 360/75 computer with a Fortran version of the programs previously used.<sup>28</sup>

### ANALYSIS OF THE RADIAL DISTRIBUTION CURVES

The radial distribution curves,  $D(r)$ , for the solutions investigated are given in Fig. 4 and the functions  $D(r) - 4\pi r^2 \rho_0$  in Fig. 5.

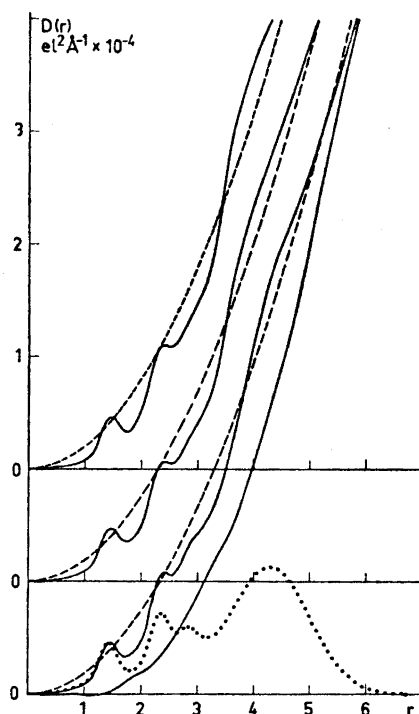


Fig. 4. Radial distribution curves,  $D(r)$ . Dashed lines are the corresponding  $4\pi r^2 \rho_0$  functions. The dotted curve is the sum of the peak shapes calculated with the use of the parameters obtained in the least squares refinement of the acid solution (Table 3). The difference between the  $D(r)$  curve and the calculated peaks for the acid solution (lower curve) is also shown.

The Cl–O interaction at 1.4 Å in the perchlorate groups is clearly seen in all the curves. The Sn–O distances within the first coordination sphere of the Sn atom are not well resolved in the  $D(r)$  curves (Fig. 4). In Fig. 5 two peaks, one at 2.3 Å and one at 2.8 Å, are indicated. The O–O interactions in the

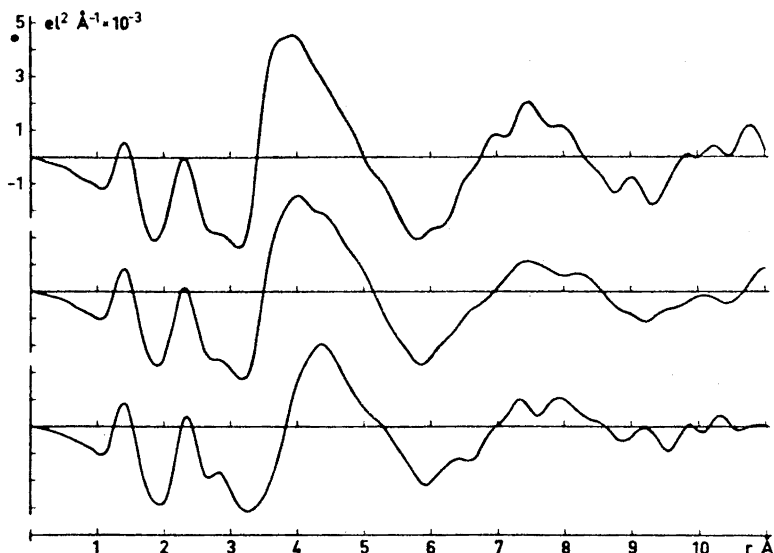


Fig. 5.  $D(r) - 4\pi r^2 \rho_0$  functions for the three solutions investigated. The lower curve represents the acid solution (I) and the upper curve the most hydrolyzed of the solutions (III).

perchlorate groups will contribute to the 2.3 Å peak, but cannot alone explain the full size of the peak. In crystals the tin(II) atom often forms three short bonds of about 2.3 Å to oxygen atoms with two or three other oxygens at distances about 0.5 Å longer.<sup>29</sup> These two peaks appear in approximately the same way in all the distribution curves and the corresponding interactions are thus largely unaffected by hydrolysis.

A broad peak at about 4.3 Å for the acid solution probably contains contributions from distances within a second coordination sphere around the tin atoms. It seems to be the only peak in the  $D(r)$  function which changes significantly when the solution is hydrolyzed. In the following treatment of the data the 2.8 Å peak and the 4.3 Å peak will both be treated as resulting from Sn—O interactions only, although they probably contain significant contributions from light-atom interactions. Remaining parts of the water structure and hydration of the perchlorate groups may be expected to give contributions in the corresponding regions.

The changes in the distribution curves with hydrolysis are more clearly brought out by the difference curves in Fig. 6. They have been obtained by subtracting from each of the  $D(r)$  functions the corresponding  $4\pi r^2 \rho_0$  function calculated for the light atoms only and then taking the differences between the resulting curves. If changes in the light atom interactions on hydrolysis are negligible, the peaks in the difference curves should be solely determined by changes in the surroundings of the tin atoms.

According to Fig. 6 only minor changes seem to occur within the first coordination sphere of the tin atoms. The peak at about 3.6 Å can probably



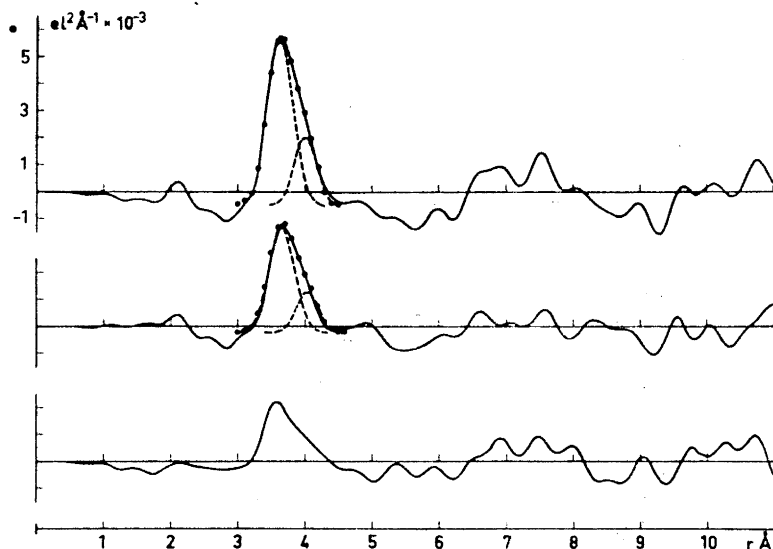


Fig. 6. Differences between the radial distribution curves. The upper curve gives the difference between the solutions with  $\bar{n}=0.8$  (III) and  $\bar{n}=0$  (I), the middle curve between the solutions with  $\bar{n}=0.5$  (II) and  $\bar{n}=0$  (I), and the lower curve gives the difference between the two hydrolyzed solutions (III–II). The dashed curves are calculated from the parameters given in the last column in Table 4. The sum of the two curves, which closely reproduces the observed peak, is marked by dots.

be correlated with Sn–Sn distances within polynuclear hydrolysis complexes. Distances between the oxygen-bridged Sn atoms within the octa-nuclear complexes in the crystals of  $\text{Sn}_2\text{OSO}_4$  range from 3.49 Å to 3.77 Å with an average value of 3.65 Å.<sup>11</sup> In  $\text{Sn}_6\text{O}_4(\text{OH})_4$  the short Sn–Sn distances within the octahedra have been reported to be 3.59 Å.<sup>13,14</sup>

The 3.6 Å peak is not symmetric but is extended towards longer distances. Non-equal Sn–Sn distances, well-defined long Sn–O distances within the hydrolysis complexes, or a general shortening of distances within the second coordination sphere when a solution is hydrolyzed, may cause this asymmetry. Comparison with calculated peak shapes for Sn–Sn interactions shows that the left side of the peak agrees well with that calculated for an Sn–Sn interaction of 3.62 Å with a temperature factor  $b=0.0083$ . If we assume that this represents a well-defined Sn–Sn distance within the complexes, its frequency in the most hydrolyzed of the solutions would correspond to an average number of about 1.2 Sn atoms bonded to each other Sn atom in the solution.

If the calculated peak shape, obtained by the best fit to the left side of the 3.6 Å peak, is subtracted from the difference curves in Fig. 6, small peaks remain at about 4 Å. The area of each of these peaks corresponds to approximately one third of that of the corresponding main peak (Table 4). If it is assumed to correspond to Sn–Sn interactions, the total number of Sn atoms bonded to each other Sn atom in the most hydrolyzed of the solutions would

Table 3. Results from the least squares refinement for the acid solution. The final values are given for the distance,  $d$  (in Å), the frequency of the distance (per Sn atom),  $n$ , and the temperature factor,  $b$ , obtained for each interaction in the different  $s$  ranges. The calculated standard deviations are given in brackets. The values in the columns  $b$  were obtained when the values of  $n$  and  $d$  for the perchlorate group, with  $d$  representing the Cl—O distance, were kept constant during the refinement.

2.8 < $s$ < 15			5.0 < $s$ < 15			7.0 < $s$ < 15			9.0 < $s$ < 15		
a			a			a			a		
b			b			b			b		
ClO <sub>4</sub>	$d$	1.410 [4]	1.406	1.410 [4]	1.406	1.405 [4]	1.406	1.406 [4]	1.406		
	$n$	0.88 [2]	1	0.90 [3]	1	0.92 [3]	1	0.99 [2]	1		
	$b$	0.000 [1]	0.0010 [3]	0.000 [2]	0.0004 [3]	0.000 [1]	0.0004 [2]	0.000 [1]	0.0004 [3]		
Sn—O	$d$	2.33 [1]	2.33 [1]	2.32 [1]	2.33 [1]	2.33 [1]	2.34 [1]		2.32 [1]		
	$n$	2.00 [10]	2.40 [15]	1.8 [2]	1.6 [3]	2.0 [2]	2.4 [4]		2.8 [15]		
	$b$	0.000 [3]	0.002 [1]	0.000 [2]	0.000 [2]	0.000 [2]	0.0009 [15]		0.003 [3]		
Sn—O	$d$	2.81 [1]	2.83 [1]	2.86 [2]	2.87 [2]	2.79 [3]					
	$n$	3.1 [2]	3.0 [1]	10.0 [10]	3.2 [16]	2.0 [8]					
	$b$	0.017 [4]	0.015 [4]	0.055 [7]	0.018 [9]	0.02 [1]					

Table 4. Results from the least squares refinements for the hydrolyzed solutions (II and III in Table 1). For each interaction the final values obtained for each  $s$  range for the distance,  $d$ , the frequency,  $n$  (= the number of interactions per Sn atom), and the temperature factor,  $b$ , are given. Contributions from the perchlorate groups and the Sn—O interactions within the first coordination sphere were assumed to be the same as for the acid solution. In the last column are given the parameters for the two Sn—Sn interactions, which were used to calculate the peak shapes in Fig. 6.

Solution No.	Type of refinement	Type of interaction	Parameter	$1.4 < s < 10.2$	$2.6 < s < 10.2$	$4.2 < s < 10.2$	$6.2 < s < 10.2$	Values obtained from the diff. curves in Fig. 6
III	A	Sn—Sn	$d$	3.672[13]	3.673[10]	3.651[10]	3.601[12]	3.62
			$n$	0.96 [4]	0.79 [5]	0.99 [23]	1.0 [4]	0.586 and 0.214
			$b$	0.036 [5]	0.024 [4]	0.035 [8]	0.027 [7]	0.0083 0.0039
		Sn—O	$d$	4.17				
			$n$	24.5 const.				
			$b$	0.22				
	B	Sn—Sn	$d$	3.681[23]	3.701[17]	3.659[11]	3.601[12]	
			$n$	0.60 [9]	1.31 [19]	0.98 [23]	1.0 [3]	
			$b$	0.017 [6]	0.041 [7]	0.036 [9]	0.027 [6]	
		Sn—O	$d$	4.09 [2]	4.42 [8]		0	
			$n$	29.0 [20]	18.7 [64]			
			$b$	0.24 [2]	0.18 [4]			
II	A	Sn—Sn	$d$	3.691[12]	3.684[10]	3.697[11]	3.615[18]	3.64
			$n$	0.51 [2]	0.53 [4]	0.78 [19]	1.3 [7]	0.386 and 0.128
			$b$	0.027 [4]	0.027 [4]	0.047 [9]	0.046[11]	0.0083 0.0039
		Sn—O	$d$	4.17				
			$n$	24.5 const.				
			$b$	0.22				
	B	Sn—Sn	$d$	3.694[20]	3.729[16]	3.696 [9]	3.61 [2]	
			$n$	0.48 [6]	1.2 [2]	0.8 [2]	1.4 [7]	
			$b$	0.025 [6]	0.054 [8]	0.05 [1]	0.05 [1]	
		Sn—O	$d$	4.17 [2]	4.47 [7]		0	
			$n$	25.4 [10]	18.1 [22]			
			$b$	0.23 [1]	0.18 [4]			

then be about 1.6 rather than 1.2. If it is assumed to represent Sn–O interactions each Sn atom would have about two oxygens at this distance.

The ratio of the sizes of the 3.6 and 4 Å peaks is approximately constant – within the rather limited precision – for all the difference curves in Fig. 6. Thus the asymmetry of the 3.6 Å peak is independent of the degree of hydrolysis, which perhaps can be taken to indicate that it is a characteristic of one single type of complex.

The curves in Fig. 6 do not show significant features, which can be interpreted as longer Sn–Sn distances than those occurring in the 3.6 to 4 Å region. However, interactions, which have frequencies much lower than that of the primary Sn–Sn distance, may well escape detection among the spurious background peaks present in the curves.

#### ANALYSIS OF THE REDUCED INTENSITY FUNCTIONS

A further analysis of the predominant interactions in the solutions was made by means of a least squares procedure applied directly to the measured intensity data.

Theoretical intensity values were calculated according to the expression

$$i(s) = \sum_n \sum_{\substack{m \\ n \neq m}} f_n f_m \sin r_{nm}s / (r_{nm}s) \exp(-b_{nm}s^2)$$

Here  $r_{nm}$  is the distance between two atoms  $n$  and  $m$ ,  $f_n$  and  $f_m$  are the scattering factors, and  $b$  is a temperature factor. For each pair interaction the distance, a temperature factor, and a frequency factor were introduced as parameters and were refined by a least squares procedure which minimized the function  $\sum s^2 [i_{\text{obs}}(s) - i_{\text{calc}}(s)]^2$ .

Because of the low atomic number of Sn the perchlorate groups contribute relatively more to the scattering than in the solutions investigated previously.<sup>15,17</sup> For this reason, the corresponding parameters were also refined with the single restriction that the tetrahedral symmetry of the  $\text{ClO}_4^-$  group was preserved. Sn–O interactions corresponding to the first coordination sphere of the tin atom and a similar interaction approximating the many distances around 4.3 Å, were also introduced, as were Sn–Sn interactions for the hydrolyzed solutions.

Results from the refinement of the scattering curve of the acid solution are given in Table 3. The broad peak at about 4.3 Å in the radial distribution curve, which was interpreted as indicating a second coordination sphere around the Sn atom, corresponds to significant contributions to the scattering curves only in the low-angle region. The corresponding interaction parameters were determined in a separate refinement, which included this region, and were then kept constant in the following refinements.

The frequencies representing the interactions within the perchlorate group and the first coordination sphere of the tin atom were refined simultaneously. In order to check the constancy of the refined parameters the lower  $s$  limit was increased continuously, as shown in Table 3. For the highest  $s$  limit only the  $\text{ClO}_4$  interactions still showed significant contributions to the observed intensity values.

The parameters obtained for the  $\text{ClO}_4$  group (columns "a" in Table 3) are interesting as a check on the experimental data and on the refinement procedure. The Cl–O distance, which was found to be 1.41 Å ( $\sigma=0.01$  Å), is independent of the  $s$  range used and is consistent with values found in crystals, which are usually around 1.43 Å.<sup>30</sup> The frequency factor does not differ significantly from the expected value of one, but comes out slightly lower than this value, particularly for the lower  $s$  limits. Here, on the other hand, the temperature factor, which was assumed to be the same for the Cl–O and the O–O interactions, comes out slightly negative (about the magnitude of the standard deviation), when not restricted to positive values only.

In a second series of refinements the frequency factor of the  $\text{ClO}_4$  interactions was assumed to have the expected value of one, and only the temperature factor was refined. These results are also given in Table 2 (columns "b").

Both the 2.3 Å and the 2.8 Å Sn–O interactions seem to represent well-defined frequencies in the scattering curves. The first gives significant contributions up to somewhat higher  $s$  values than does the second. Each of them corresponds to between two and three oxygens bonded to each tin atom. However, the precision of these determinations, as shown by the standard deviations, is low.

The comparison between the radial distribution curves (Fig. 6) shows only minor changes to occur within the first coordination sphere of the tin atom when a solution is hydrolyzed. For the refinements of the scattering curves from the hydrolyzed solutions, therefore, the same parameters were used as those found for the acid solution and only the parameters for a single Sn–Sn interaction at about 3.6 Å were refined.

Although the 3.6 Å interaction and the interactions from the second coordination sphere at about 4.2 Å are not resolved in the distribution curves (Fig. 5), they can be resolved by the least squares procedure. Two series of refinements were made for which the results are given in Table 4. In the first series (A) only the three parameters for an Sn–Sn interaction at about 3.6 Å were refined, keeping the other parameters constant at the values found for the acid solution. In the second series (B) the three parameters corresponding to Sn–O interactions from the second coordination sphere were refined in addition to those of the Sn–Sn interactions. In the first series values for the number of Sn–Sn interactions are obtained which, as expected, do not differ significantly from those estimated from the areas under the peaks in Fig. 6. Also in the second series these values come out with about the same magnitude. The precision is low, however, as shown by the standard deviations.

The results from the least squares refinements thus support the conclusions that the peaks in the difference curves in Fig. 6 are of a different character than those of the second coordination sphere and thus probably result from well-defined interactions within polynuclear complexes and not from changes in light atom positions in the second coordination sphere.

#### DISCUSSION OF THE RESULTS

The agreement between observed and calculated  $s \cdot i(s)$  values are shown in Fig. 3. The contributions of each interaction to the  $s \cdot i(s)$  curve and the  $D(r)$  curve are shown in Fig. 7 for the most hydrolyzed of the solutions.

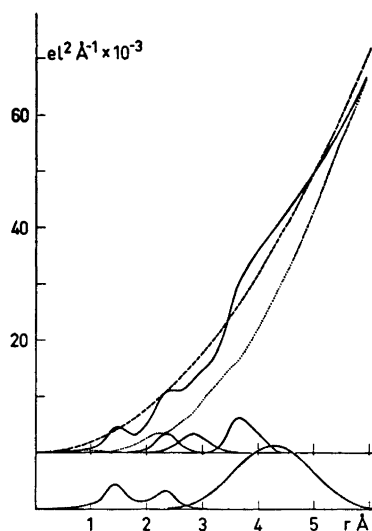
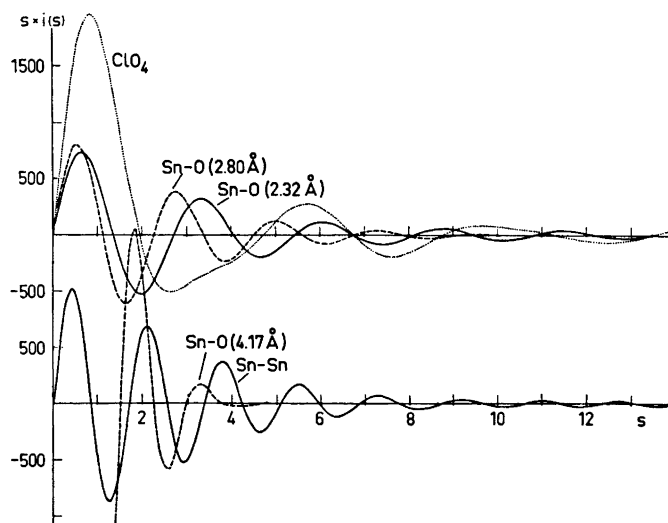


*Fig. 7.* The contributions of the different interactions to the  $s \cdot i(s)$  and the  $D(r)$  curves for the most hydrolyzed of the solutions (III). The following parameter values (distance, frequency factor, temp. factor) have been used:  $\text{ClO}_4$ : 1.406 (Cl—O), 1, 0.0008; Sn—O: 2.32, 2.3, 0.0013; 2.80, 3.0, 0.015; 4.17, 24.5, 0.22; Sn—Sn: 3.62,  $0.59 \times 2$ , 0.0083 and 4.00,  $0.21 \times 2$ , 0.0039. The experimental  $D(r)$  curve, the corresponding  $4\pi r^2 \rho_0$  function, and the difference curve obtained by subtracting the calculated peak shapes from the  $D(r)$  function are also shown.

At the larger scattering angles only the perchlorate groups make significant contributions to the reduced intensities. Interactions involving the tin atoms have a relatively minor influence. Two well-defined peaks, at 2.3 Å and at 2.8 Å in the radial distribution curves can, however, be related to Sn–O interactions within the first coordination sphere. The least squares analysis of the intensity curves (Table 3) show them to correspond to well-defined frequencies, each with an amplitude of a magnitude expected for two to three Sn–O contacts per Sn atom. The tin atom, therefore, may have two groups of coordinated water molecules, one of which is more strongly bonded than the other.

The less strongly bonded oxygens occur at a distance where light-atom contacts begin to dominate, such as O–O and, in the hydrolyzed solutions, Na–O contacts, and these may contribute to, or even fully explain, the 2.8 Å peak. The conclusion that the tin atom may have two groups of neighbouring water molecules is, however, in agreement with results from crystal structure determinations, where the tin atom is often found to have about three oxygens at approximately 2.3 Å with some other oxygens at longer distances. The same coordination of the Sn atom is found for all the three solutions investigated and thus it is not noticeably dependent on the degree of hydrolysis.

The Sn–Sn distances within the expected polynuclear hydrolysis complexes are less well-defined. The detailed analysis of the distribution curves and the reduced intensity functions shows, however, that such interactions are present in the 3.6 to 4 Å region. In crystals Sn–Sn distances within polynuclear complexes have also been found to be of this magnitude.<sup>11,13,14</sup>

The analysis of the experimental data indicates that the Sn–Sn distances may be slightly different, varying between 3.6 and 4 Å, which makes the estimate of the frequency of the distances more difficult and less accurate. For the most hydrolyzed of the solutions, however, the analysis of the results shows conclusively, that the average number of Sn atoms bound to each other

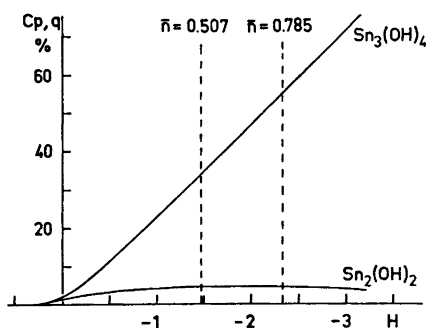


Fig. 8. Fraction of tin(II) bound in the different hydrolysis complexes,  $\text{Sn}_q(\text{OH})_p^{(2q-p)+}$ , as calculated from the equilibrium constants given by Tobias.<sup>7</sup>

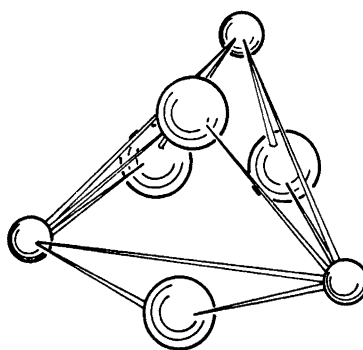


Fig. 9. Possible structure for a tri-nuclear hydrolysis complex. Small circles denote Sn(II) atoms and large circles oxygen atoms.

Sn atom in the solution is larger than one. Thus complexes containing more than two Sn atoms must be formed.

Expected concentrations of hydrolysis complexes as calculated from the stability constants given by Tobias<sup>7</sup> are shown in Fig. 8. The tri-nuclear complex  $\text{Sn}_3(\text{OH})_4^{2+}$  is seen to be predominant, but as the maximum concentration used by Tobias was 0.04 M compared to the 3 M concentrations used here, the constants used may not even approximately be valid for the present solutions.

Several authors have suggested a triangular structure for an  $\text{Sn}_3(\text{OH})_4^{2+}$  complex as shown in Fig. 9.<sup>7,29</sup> The Sn—Sn distances expected for this structure are consistent with those found from the X-ray scattering and so is — within the very limited accuracy — the expected degree of condensation, as is the absence of longer Sn—Sn distances in the distribution curves. Although Sn—O distances in such a structure would fall in the region around 4 Å and would thus, at least in part, explain the asymmetry of the peaks in the difference curves in Fig. 6, it seems that the Sn—Sn distances would still have to be slightly different in order to explain the experimental data. For a simple triangular complex, equal Sn—Sn distances would seem more likely and a well-defined frequency in the scattering curves with significant Sn—Sn contributions up to much higher *s* values than those now found would rather be expected for a predominant triangular complex.\*

The octa-nuclear complexes found in crystals of  $\text{Sn}_2\text{OSO}_4$  and built up from tetrahedra of Sn atoms sharing faces have been shown to have non-equal Sn—Sn distances ranging from 3.486 Å to 3.772 Å.<sup>11</sup> Non-equal metal-metal distances have also been found in the similarly constructed hexa-nuclear  $\text{Pb}_6\text{O}(\text{OH})_6^{4+}$  complex, where the Pb—Pb distances range from 3.45 Å to 4.09 Å.<sup>12</sup> In complexes of this type longer metal-metal distances would also occur, but would have a much lower frequency than the primary distance and may therefore, if such complexes occur in the solutions, escape detection in the radial distribution curves. An alternative explanation to non-equal Sn—Sn distances would, of course, be the occurrence of several complexes in the solutions, having different structures and therefore slightly different Sn—Sn distances.

## CONCLUSIONS

We can conclude from the X-ray scattering data that hydrolysis of tin(II) perchlorate solutions leads to the formation of polynuclear complexes with Sn—Sn distances around 3.6 Å. This condensation of the hydrated tin(II) ions, when protons are dissociated, does not stop at dinuclear complexes since in the most hydrolyzed of the solutions investigated (Table 1), the average number of Sn atoms bonded to each other Sn atom is larger than one. These polynuclear complexes probably contain the same type of  $\text{OSn}_3$  groups, with a triangular arrangement of the Sn atoms, which has been found in crystals

\* In a preliminary note<sup>31</sup> on the crystal structure of  $\text{Sn}_3\text{O}(\text{OH})_2\text{SO}_4$  it has been reported that this structure contains discrete  $\text{Sn}_3\text{O}(\text{OH})_2^{2+}$  units with non-equal Sn—Sn distances. The distances found were 4.063 Å, 4.209 Å, and 4.605 Å and thus differ considerably from those in the present work and in crystal structures of other basic Sn(II) salts.<sup>11,13,14</sup>



of  $\text{Sn}_2\text{OSO}_4$ <sup>11</sup> and  $\text{Sn}_6\text{O}_4(\text{OH})_4$ .<sup>13,14</sup> This is indicated by the close similarity of the Sn—Sn distances in the crystals and in the solutions and by the absence of clearly marked longer Sn—Sn distances in the radial distribution curves. We can also conclude, from the absence of clearly marked longer Sn—Sn distances, that if larger complexes than trinuclear ones would be predominant in the solutions, the  $\text{OSn}_3$  groups are probably joined into tetrahedra of the type found in  $\text{Sn}_2\text{OSO}_4$ <sup>11</sup> and not into octahedra as found in  $\text{Sn}_6\text{O}_4(\text{OH})_4$ .<sup>13,14</sup>

The X-ray data cannot distinguish between triangular and tetrahedral complexes, and even larger complexes with low-frequency longer Sn—Sn distances cannot be definitely excluded. Although the emf measurements by Tobias<sup>7</sup> make a trinuclear complex with the structure shown in Fig. 9 the most likely one, equilibrium measurements on more concentrated solutions than those used by Tobias<sup>7</sup> are needed before definite conclusions about the structures can be made.

*Acknowledgements.* The work has been supported by *Statens Naturvetenskapliga Forskningsråd* (Swedish Natural Science Research Council). Computer time has been made available by the *Computer Division of the National Swedish Office for Administrative Rationalization and Economy*.

We thank Miss Anita Johansson for assistance in the work and Dr. Derek Lewis for linguistic corrections.

#### REFERENCES

1. Prytz, M. *Z. anorg. Chem.* **174** (1928) 355.
2. Randall, M. and Murakami, S. *J. Am. Chem. Soc.* **52** (1930) 3967.
3. Gorman, M. *J. Am. Chem. Soc.* **61** (1939) 3342.
4. Garrett, A. B. and Heiks, R. E. *J. Am. Chem. Soc.* **63** (1941) 562.
5. Vanderzee, C. E. and Rhodes, D. E. *J. Am. Chem. Soc.* **74** (1952) 3552.
6. Vanderzee, C. E. and Rhodes, D. E. *J. Am. Chem. Soc.* **74** (1952) 4806.
7. Tobias, R. S. *Acta Chem. Scand.* **12** (1958) 198.
8. Olin, Å. *Acta Chem. Scand.* **14** (1960) 126.
9. Olin, Å. *Acta Chem. Scand.* **14** (1960) 814.
10. Pajdowski, L. and Olin, Å. *Acta Chem. Scand.* **16** (1962) 983.
11. Wernfors, G. *Acta Chem. Scand.* **15** (1961) 1007.
12. Spiro, T. G., Templeton, D. H. and Zalkin, A. *Inorg. Chem.* **8** (1969) 856.
13. Howie, R. A. and Moser, W. *Nature* **219** (1968) 372.
14. Söderqvist, R. *Personal communication*.
15. Johansson, G. and Olin, Å. *Acta Chem. Scand.* **22** (1968) 3197.
16. Johansson, G. *Acta Chem. Scand.* **22** (1968) 399.
17. Johansson, G. *Acta Chem. Scand.* **25** (1971) 2787.
18. Åberg, M. *Acta Chem. Scand.* **24** (1970) 2901.
19. Noyes, A. and Toabe, R. *J. Am. Chem. Soc.* **39** (1917) 1537.
20. Jamieson, G. S. *Volumetric Iodate Methods*, The Chemical Catalog Co., New York 1926, p. 75.
21. Gran, G. *Analyst* **77** (1952) 661.
22. Johansson, G. *Acta Chem. Scand.* **20** (1966) 553.
23. Cromer, D. T. and Waber, J. T. *Acta Cryst.* **18** (1965) 104.
24. Cromer, D. T. *Acta Cryst.* **18** (1965) 17.
25. *International Tables for X-Ray Crystallography*, Kynoch Press, Birmingham 1962, Vol. III.
26. Compton, A. H. and Allison, S. K. *X-Rays in Theory and Experiment*, Van Nostrand, New York 1935.
27. Bewilogua, L. *Phys. Z.* **32** (1931) 740.

28. Johansson, G. Programs with Accession Nos. 6037 and 6038 in *IUCr World List of Crystallographic Computer Programs*, 2nd Ed., London 1966.
29. Donaldson, J. D. *Progr. Inorg. Chem.* **8** (1967) 287.
30. *Tables for Interatomic Distances and Bond Angles*, Special Publication No. 18, The Chemical Society, London 1965, p. 58.
31. Davies, C. G. and Donaldson, J. D. *Acta Cryst. A* **25** (1969) 122, 8th IUCr. Suppl.

Received July 17, 1972.